

## Electrical resistivity studies of Cr - Ir alloy single crystals

This article has been downloaded from IOPscience. Please scroll down to see the full text article.

1996 J. Phys.: Condens. Matter 8 10473

(<http://iopscience.iop.org/0953-8984/8/49/035>)

View [the table of contents for this issue](#), or go to the [journal homepage](#) for more

Download details:

IP Address: 171.66.16.207

The article was downloaded on 14/05/2010 at 05:50

Please note that [terms and conditions apply](#).

## Electrical resistivity studies of Cr–Ir alloy single crystals

J Martynova, H L Alberts and P Smit

Department of Physics, Rand Afrikaans University, PO Box 524, Auckland Park, Johannesburg 2006, South Africa

Received 17 June 1996

**Abstract.** Electrical resistivity has been measured for four Cr–Ir alloy single crystals for concentrations between 0.07 and 0.25 at.% Ir in the temperature range 4 to 1200 K. Well defined magnetic anomalies were observed at the Néel temperature ( $T_N$ ) of each alloy as well as at the incommensurate–commensurate (I–C) spin-density-wave (SDW) phase transition temperature of a Cr + 0.20 at.% Ir alloy. The latter transition is hysteretic, of hysteresis width about 20 K, which is indicative of a first-order ISDW–CSDW phase transition. Analyses of the data show that the fraction of the electron and hole Fermi surface sheets that nests is roughly the same in the ISDW and CSDW phases. A magnetic contribution to the resistivity, amounting to between 20% and 25% of the total resistivity at the Néel point, is observed in the alloys. This contribution, probably due to spin-fluctuation effects, persists to temperatures well above  $T_N$ , up to about  $2.5T_N$ .

### 1. Introduction

Cr and its dilute alloys are spin-density-wave (SDW), itinerant-electron antiferromagnets [1]. The SDW originates from nesting between parts of the electron and hole Fermi surface sheets, centred respectively at points  $\Gamma(0, 0, 0)$  and  $H(1, 0, 0)$  of  $k$ -space [2]. The Coulomb interaction between electrons and holes on these two nesting surfaces gives rise to electron–hole condensation into the SDW state and to a resultant formation of energy gaps on or near the Fermi surface at temperatures below the Néel temperature,  $T_N$  [1, 2]. The appearance of these energy gaps has a marked influence on the electrical resistivity,  $\rho$ , just below  $T_N$ , giving rise to an increase in  $\rho$ , followed by a peak value, on lowering the temperature through  $T_N$ . Electrical resistivity measurements on Cr and its dilute alloys therefore give valuable information regarding the SDW in these materials.

In pure Cr the  $Q$ -vector of the SDW, directed along a [100] or equivalent direction, is not commensurate with the lattice, giving rise to an incommensurate (I) SDW state below  $T_N$ . The ISDW phase in Cr is transformed to a commensurate (C) SDW phase by alloying Cr with small amounts of elements like Mn, Pt, Ru, and Ir [1]. These alloys then have a triple point, at concentration  $c_t$ , on their magnetic phase diagrams where three magnetic phases, the paramagnetic (P) phase and the ISDW and CSDW phases, coexist [1]. For  $c < c_t$  the alloy remains in the ISDW phase at all  $T < T_N$  while two SDW phases appear below  $T_N$  for  $c > c_t$ , namely the CSDW phase for  $T_{IC} < T < T_N$  and the ISDW phase for  $T < T_{IC}$ , where  $T_{IC}$  is the ISDW–CSDW phase transition temperature.

In nearly all electrical resistivity studies done up to now on dilute polycrystalline Cr alloys the ISDW–P and CSDW–P phase transitions were found to be characterized by well defined magnetic anomalies on the  $\rho$ – $T$  curves near  $T_N$  [1]. For the ISDW–CSDW phase

transition, however, conflicting data appear in the literature concerning the appearance or non-appearance of a magnetic anomaly at  $T_{IC}$ . For dilute Cr–Ru alloys for instance, some authors [3] observed no  $\rho$ -anomaly near  $T_{IC}$  in conflict with the measurements of others [4, 5] who did observe a small anomaly near this temperature. The same applies to dilute Cr–Ir alloys. Studies by de Young *et al* [6] and by Yakhmi *et al* [7] on polycrystalline dilute Cr–Ir alloys show no magnetic anomaly at  $T_{IC}$  for this alloy system while measurements of Butylenko and Nevdacha [4] show an anomaly in their  $\rho$ – $T$  data when their Cr–Ir samples are heated at a rate of 4 to 5 K min<sup>−1</sup> through  $T_{IC}$ . There is however a problem with the measurements of Butylenko and Nevdacha [4]. At  $T > T_N$  we estimate from their data  $d\rho/dT \approx 0.02 \mu\Omega \text{ cm K}^{-1}$  for pure Cr and for their dilute Cr alloys (they show curves for Cr–Ru only), which is rather low compared to  $d\rho/dT \approx 0.04 \mu\Omega \text{ cm K}^{-1}$  obtained in other studies [8, 9] on pure Cr. Below  $T_N$ ,  $d\rho/dT$  of Butylenko and Nevdacha [4] for Cr is comparable to that obtained from the data of the other studies [8, 9].

Nesting between the electron and hole Fermi surface sheets is expected to improve when the SDW transforms from the incommensurate to the commensurate state in Cr–Ir alloys with  $c > c_t$  [1]. This should lead to a larger truncation of the Fermi surface in the CSDW phase than in the ISDW phase and therefore to a magnetic anomaly in  $\rho$  at  $T_{IC}$  as well as to a larger  $\rho$  anomaly at  $T_N$ , compared to the case for alloys with an ISDW–P Néel transition.

In previous studies [6, 7] on Cr–Ir alloys, the magnetic anomaly in the resistivity

$$\frac{\Delta\rho(T)}{\rho(T)} = \frac{\rho(T) - \rho_P(T)}{\rho(T)}$$

at  $T < T_N$  where  $\rho_P$  is the expected resistivity at the same temperature in the absence of magnetic ordering, was determined by a linear extrapolation of the  $\rho$ – $T$  curve from the paramagnetic region down to the antiferromagnetic region.  $\Delta\rho(0)/\rho(0)$  is a measure [10, 11] of the fraction of the Fermi surface that is truncated by the formation of the SDW energy gap below  $T_N$ . Studies of Chiu *et al* [11] however show that a simple linear extrapolation is not good enough for an accurate analysis of the electrical resistivity of dilute Cr alloys. The reason is that magnetic excitations in these alloys may exist [1] to temperatures as high as  $1.5T_N$  or higher, suggesting very large precursor effects. It is therefore necessary to study  $\rho$ – $T$  curves of dilute Cr–Ir alloys to temperatures well above  $T_N$  for a detailed analyses. In this regard it may be mentioned that the measurements of Yakhmi *et al* [7] on Cr–Ir alloys were done only to temperatures up to about  $1.35T_N$  or less, which is not high enough to determine accurately the non-magnetic component of  $\rho$  at  $T < T_N$  by back-extrapolation. The resistivity measurements of de Young *et al* [6] were to high enough temperatures but they analyse their data using a linear back-extrapolation from high temperatures and their data furthermore show no  $\rho$ -anomaly at  $T_{IC}$ . We report here  $\rho$ – $T$  measurements up to  $\approx 1200$  K on four Cr–Ir alloy single crystals, one with  $c < c_t$ , one with  $c$  very close to  $c_t$  and two with  $c > c_t$ . The data are analysed using the techniques first used by Chiu *et al* [11].

## 2. Experimental procedure

The Cr–Ir alloy single crystals were grown by a floating-zone technique using radio-frequency heating as previously described [12] for the growth of other Cr alloy single crystals. The starting materials were polycrystalline rods prepared from 99.996% pure Cr and 99.9% pure Ir. The actual concentrations of 0.07 at.% Ir, 0.17 at.% Ir, 0.20 at.% Ir and 0.25 at.% Ir for the four crystals were determined using electron microprobe analysis techniques. The error in the absolute value of these concentrations is about 20 to 25%.

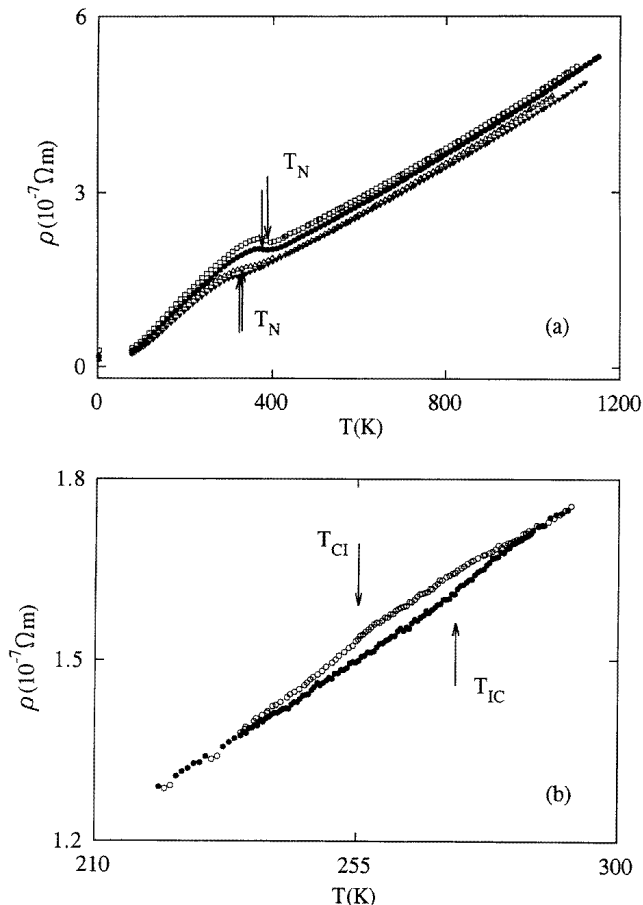


**Figure 1.** (a) Electrical resistivity,  $\rho$ , as a function of temperature for Cr-Ir alloy single crystals. Measurements were done on slowly heating the sample at a rate of less than  $0.5 \text{ K min}^{-1}$  and data were recorded at  $0.05 \text{ K}$  intervals. For clarity not all of the data points are shown. Data points are marked as follows:  $\blacktriangledown$ : 0.07 at.% Ir,  $\triangle$ : 0.17 at.% Ir,  $\bullet$ : 0.20 at.% Ir and  $\square$ : 0.25 at.% Ir. For the samples containing 0.07 and 0.20 at.% Ir the current was directed along [100] while it was directed along [110] for the other two samples. (b) Electrical resistivity,  $\rho$ , for both cooling and heating runs for Cr + 0.20 at.% Ir near  $T_{CI}$  (on cooling  $\circ$ ) and  $T_{IC}$  (on heating  $\bullet$ ). Data were recorded at  $0.05 \text{ K}$  intervals and not all of the data points are shown, for clarity.

Electrical resistivity was measured using a standard four-probe DC method for both forward and reverse current directions in order to eliminate thermal emfs. The sample lengths were about 8 mm and the cross sectional area about  $1 \text{ mm}^2$ . The longest axis was directed either along [100] or [110], depending on which direction in the crystal gives the longest length. The Cr-Ir crystals in this study were in the multi- $Q$ -domain state [2], meaning that they consist of magnetic domains below  $T_N$  in which the SDW  $Q$ -vector in each is directed at random along any one of the six equivalent [100] directions. Furthermore, since the crystals are of cubic structure and electrical conductivity is represented by a tensor of the second rank, we do not expect [13] anisotropy of the electrical resistivity in these alloys. Current was applied along the long axis of the sample and data were recorded during both heating

and cooling runs in the temperature range 77 to 1200 K as well as at a constant temperature of 4.2 K. During heating runs from 77–1200 K data were recorded at  $\approx 0.05$  K intervals while heating the sample slowly at less than  $0.5$  K  $\text{min}^{-1}$ . The cooling rate was the same and data were recorded at the same intervals.

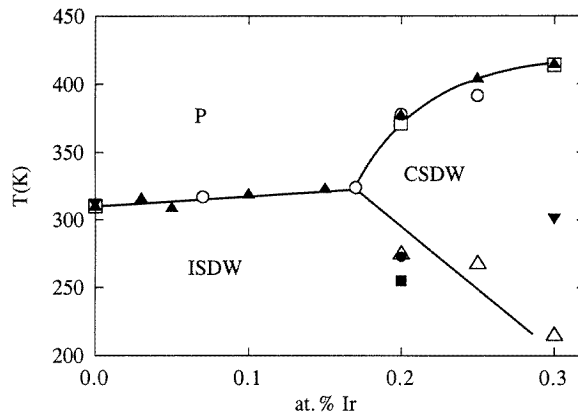


**Figure 2.** The magnetic phase diagram of dilute Cr–Ir alloys. Points marked  $\circ$  are values of the Néel temperature from this study and the points  $\bullet$  and  $\blacksquare$  are, respectively, values for  $T_{IC}$  and  $T_{CI}$  also from this study. Points marked  $\blacktriangledown$  are for  $T_N$ -values from reference [6], those marked  $\blacktriangle$  are from reference [4] for  $T_N$ , those marked  $\triangle$  are from reference [4] for  $T_{IC}$  and those marked  $\square$  are from reference [7] for  $T_N$ . The smooth curves are guides to the eye.

### 3. Results

Figure 1(a) shows  $\rho$  as a function of temperature on heating between 77–1200 K as well as values obtained at 4.2 K. Figure 1(b) shows the detailed behaviour observed during cooling and heating near the ISDW–CSDW phase transition temperature of the Cr + 0.20 at.% Ir alloy crystal. All of the samples show well defined  $\rho$ -anomalies near  $T_N$  (figure 1) with an increasing resistivity anomaly as the Ir concentration is increased. No hysteresis effects were observed at the Néel transition. The Néel temperatures, taken [1] at the inflection point just below the minimum on the  $\rho$ - $T$  curves, are shown on the magnetic phase diagram of figure 2. Also shown on this diagram are results obtained by Butylenko and Nevdacha [4], by de Young *et al* [6] and by Yakhmi *et al* [7]. Our results compare well with theirs. Figure 1(b) shows a small anomaly for Cr + 0.20 at.% Ir at the ISDW–CSDW transition with hysteresis of about 20 K, suggesting a first-order transition. The transition temperatures obtained at the inflection points shown in figure 1(b) are  $T_{IC} = 273 \pm 3$  K (on heating) and  $T_{CI} = 255 \pm 3$  K (on cooling) and are also plotted in figure 2. This behaviour is very similar to that observed in a Cr + 0.3 at.% Ru alloy single crystal [5] for which neutron diffraction experiments [14] show the ISDW–CSDW transition to be first order. We observed no effects of the ISDW–CSDW phase transition on the  $\rho$ - $T$  curve of the Cr + 0.25 at.% Ir crystal. This is probably due to the smearing out of the small anomaly at  $T_{IC}$  and  $T_{CI}$  in this crystal due to sample inhomogeneities. In fact, electron microprobe analyses at about 100 points on the two crystals, containing 0.20 and 0.25 at.% Ir, from which the electrical resistivity samples were cut, show that the former crystal is of better homogeneity than the latter. The 0.25 at.% Ir crystal was found to have a fraction of about one third of its volume

through which the average concentration was about 10% lower than that in the rest of the crystal.

#### 4. Discussion

The electrical resistivity of the dilute Cr–Ir alloy single crystals will be analysed using the methods applied by Chiu *et al* [11] to dilute Cr–Ti alloys. In their approach the electrical resistivity of a Cr alloy is given by

$$\rho_{\text{exp}}(T) = \frac{\rho_I^P}{1 - \alpha \Delta(T)/\Delta(0)} + \frac{\rho_{e-p}^P(T)}{1 - \alpha \Delta(T)/\Delta(0)} + \frac{\rho_m(T)}{1 - \alpha \Delta(T)/\Delta(0)}. \quad (1)$$

In this equation the first term represents the impurity resistivity, the second term the resistivity due to electron–phonon scattering and the last term is due to spin fluctuations that may be important at around  $T_N$ .

The factor  $[1 - \alpha \Delta(T)/\Delta(0)]^{-1}$  in each term of equation (1) appears due to the fact that the effective number of current carriers is reduced when the SDW is formed below  $T_N$ , with the concomitant appearance of the energy gaps in the electron excitation spectrum on or near the Fermi surface. It is known [11] that the SDW energy gap has a temperature dependence which is very similar to the temperature dependence of the superconducting gap in the BCS theory. Chiu *et al* [11] therefore assume that the effective number of carriers is given by  $n_{\text{eff}} = n[1 - \alpha \Delta(T)/\Delta(0)]$ , where  $\Delta(T)/\Delta(0)$  is the BCS energy gap function as tabulated by Mühlischlegel [15].  $\rho_I^P$  would be the temperature-independent impurity scattering resistivity of the Cr alloy if it was non-magnetic at all temperatures  $T > 0$  K. Similarly,  $\rho_{e-p}^P$  is the electron–phonon resistivity of the ideal non-magnetic Cr alloy and is of the form

$$\rho_{e-p}^P = \frac{k}{\theta_D^2} TG(\theta_D/T) + BT^3 \quad (2)$$

which includes [11] an electron s–d scattering term that is of importance for Cr alloys. Here  $\theta_D$  is the Debye temperature,  $G$  the Grüneisen function [16] and  $k$  and  $B$  are constants. These two constants are determined from plots of  $\rho/T^3$  versus  $1/T^2$  which are linear at temperatures well above the precursor region,  $T \gg \theta_D$ .  $\alpha$  in equation (1) is a fitting parameter which typically has a value  $\alpha \approx 0.3$  [1, 11]. At  $T = 0$  K,  $\rho_I^P = \rho_{\text{exp}}(0)(1 - \alpha)$  in equation (1) is the temperature-independent impurity resistivity of the ideal non-magnetic alloy.

In analysing our data we used equation (2) to extrapolate the  $\rho$ – $T$  curve of each Cr–Ir alloy from high temperatures down to 0 K in order to obtain the  $\rho$ – $T$  behaviour of the particular alloy that would be seen if it was to remain paramagnetic at all  $T > 0$  K. To do so we used  $\theta_D(T)$  of a Cr + 5 at.% V alloy, that remains [1] paramagnetic at all  $T > 0$  K, in equation (2). The temperature dependence of the physical properties of Cr + 5 at.% V is often used [1] to represent that of the corresponding property of the expected ideal non-magnetic state of antiferromagnetic dilute Cr alloys.  $\theta_D(T)$  was calculated, using standard techniques, from longitudinal and shear ultrasonic wave velocities measured [17] at different temperatures on a Cr + 5 at.% V alloy in our laboratory. Curves of  $[\rho_{\text{exp}}(T) - \rho_I^P]/T^3$  versus  $1/T^2$ , where  $\rho_{e-p}^P$  in equation (2) at high temperatures is given by  $\rho_{\text{exp}}(T) - \rho_I^P$  with  $\rho_I^P = \rho_{\text{exp}}(4 \text{ K})(1 - \alpha)$ , were found to be straight lines in the range  $800 < T < 1200$  K for  $\alpha$  ranging from 0.20 to 0.35, which are typical  $\alpha$ -values for dilute Cr alloys [11]. These straight lines allowed us to determine  $k$  and  $B$  in equation (2) for the back-extrapolation of the ideal non-magnetic alloy. An example of the back-extrapolation,

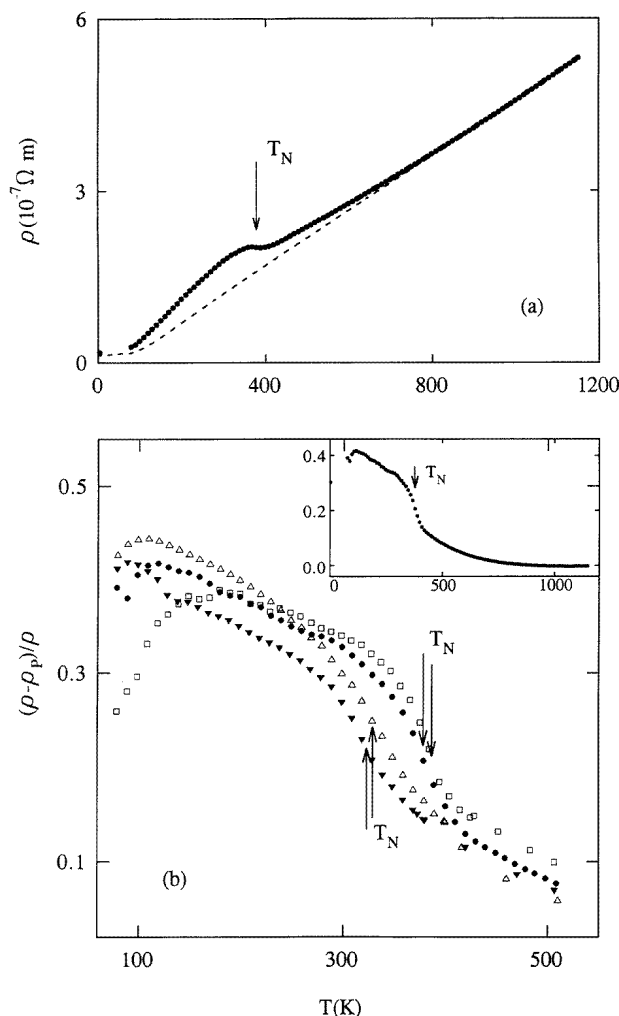


**Figure 3.** (a) An example of the back-extrapolation of the ideal non-magnetic resistivity of an alloy containing 0.20 at.% Ir. The back-extrapolation was done using equation (2) with  $\rho_{e-p}^p = \rho_{\text{exp}}(T) - \rho_I^p$  at high temperatures and using  $\alpha = 0.3$ . The broken line shows the back-extrapolation and the points  $\bullet$  are experimental points. (b) The resistivity anomaly  $(\rho - \rho_P)/\rho$  as a function of temperature for Cr-Ir alloys containing 0.07 at.% Ir ( $\blacktriangledown$ ), 0.17 at.% Ir ( $\triangle$ ), 0.20 at.% Ir ( $\bullet$ ) and 0.25 at.% Ir ( $\square$ ), all calculated with  $\alpha = 0.3$ . The inset shows as an example the behaviour over a wider temperature range for the alloy containing 0.20 at.% Ir. Here  $\rho$  is the resistivity at temperature  $T$  of the alloy and  $\rho_P$  is the resistivity that would be found at the same temperature if the alloy was non-magnetic at that temperature.

$\rho_P(T) = \rho_{e-p}^p(T) + \rho_I^p$ , is shown with  $\alpha = 0.3$  for the Cr + 0.20 at.% Ru crystal in figure 3(a).  $\Delta\rho(T)/\rho(T) = (\rho(T) - \rho_P(T))/\rho(T)$ , where the notation  $\rho(T) = \rho_{\text{exp}}(T)$  is used, for each sample with  $\alpha = 0.3$  is shown in figure 3(b). It is clear from this figure that precursor effects persist to temperatures well above  $T_N$ .  $\Delta\rho(0)/\rho(0) \approx \Delta\rho(4 \text{ K})/\rho(4 \text{ K})$  which gives a measure of the fraction of the Fermi surface that is annihilated by the formation of the SDW state, was determined for each Cr-Ir alloy for  $\alpha = 0.20, 0.25, 0.3$  and  $0.35$ . The interesting point about the  $\Delta\rho(0)/\rho(0)$  values obtained for each value of  $\alpha$  is that they

are constant within about 2%, which is within the experimental error, for the four Cr-Ir alloys. As an example  $\Delta\rho(0)/\rho(0) = 0.305, 0.305, 0.304$  and  $0.302$  for the four Cr-Ir alloys containing respectively 0.07 at.% Ir, 0.17 at.% Ir, 0.20 at.% Ir and 0.25 at.% Ir with  $\alpha = 0.3$ . This shows that the fraction of the Fermi surface sheets that nest is about the same for ISDW and CSDW Cr-Ir alloys, explaining why the  $\rho$ -anomaly at the ISDW-CSDW transition in these alloys is so small (figure 1(b)) or non-existent (as for the Cr + 0.25 at.% Ir alloy, although sample inhomogeneities probably also play a role in the latter alloy). As an example of the variation of  $\Delta\rho(0)/\rho(0)$  for the different values of  $\alpha$ , we may mention that for the Cr + 0.20 at.% Ir alloy it varies from 0.204 for  $\alpha = 0.2$  to 0.354 for  $\alpha = 0.35$ .

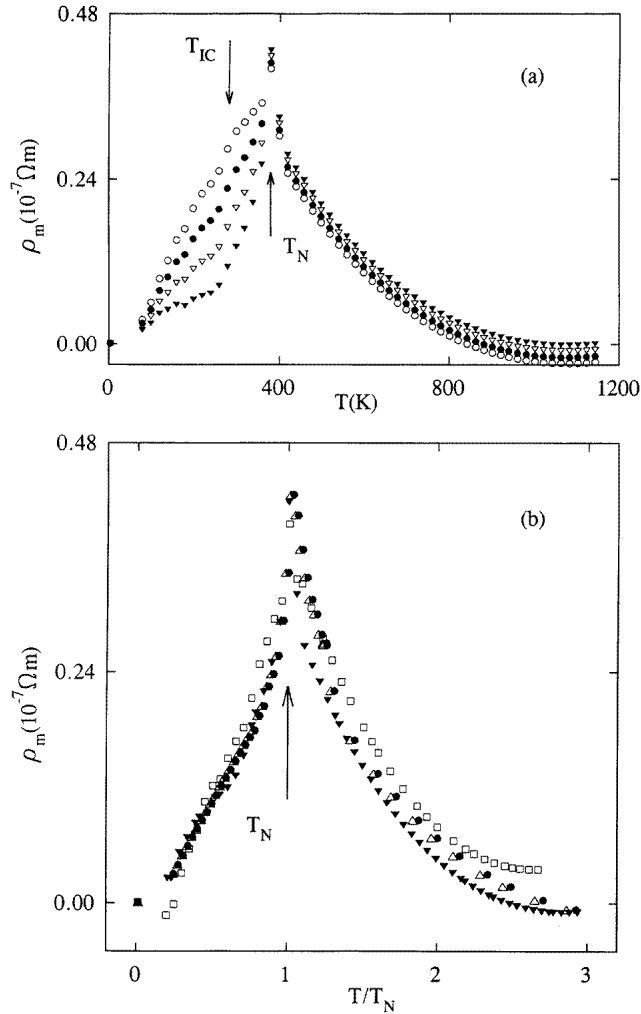


**Figure 4.** (a) The contribution  $\rho_m$  to the resistivity, equation (1), as a function of temperature for the Cr-Ir alloy containing 0.20 at.% Ir for different values of  $\alpha$ . The symbols are as follows:  $\circ$ ,  $\alpha = 0.2$ ;  $\bullet$ ,  $\alpha = 0.25$ ;  $\nabla$ ,  $\alpha = 0.3$ ; and  $\blacktriangledown$ ,  $\alpha = 0.35$ . (b) The contribution  $\rho_m$  to the resistivity for the case  $\alpha = 0.3$  in equation (1), as a function of reduced temperature,  $T/T_N$ , for Cr-Ir alloys containing 0.07 at.% Ir ( $\blacktriangledown$ ), 0.17 at.% Ir ( $\triangle$ ), 0.20 at.% Ir ( $\bullet$ ) and 0.25 at.% Ir ( $\square$ ).



The resistivity  $\rho_m(T)$ , which is thought [1] to be due to effects of spin fluctuations, was calculated using equation (1) and is shown for the Cr+0.20 at.% Ir alloy for different values of  $\alpha$  in figure 4(a). Figure 4(b) shows  $\rho_m(T)$  for the case  $\alpha = 0.3$  for the four different Cr–Ir alloys. The important points from figure 4 are that the spin-fluctuation effects are largest at  $T_N$ , as expected, that they show only a relatively small  $\alpha$ -dependence at  $T > T_N$  and that they persist to temperatures well above  $T_N$ . For  $T < T_N$ ,  $\rho_m(T)$  is dependent on  $\alpha$ : the larger  $\alpha$  the more rapidly the spin-fluctuation effects die out with decreasing  $T$ . One expects the spin-fluctuation contribution to the resistivity to die out rapidly as  $T$  decreases below  $T_N$ . The fact that, depending on the value of  $\alpha$ , it seems to persist to very low temperatures (figure 4) may be attributed to inadequacies of the model used [11].

In dilute Cr–Os alloys it was found [1, 18] that  $\Delta T = T_H - T_N$ , where  $T_H$  is the temperature that signals the onset of a linear temperature dependence of  $\rho$  at high temperatures, peaks at an Os concentration close to the triple-point concentration  $c_t$ . The presence of the peak was explained [1, 18] as due to critical conditions for the coexistence of several phases that may exist near the triple-point concentration, with the resultant fluctuations that may extend to higher temperatures in the paramagnetic phase. As Ir, like Os, is also a member of the group-8 non-magnetic transition metals of the periodic table, one expects a similar behaviour for the Cr–Ir system. However, we found  $\Delta T = 440 \pm 20$  K, being approximately constant for the four Cr–Ir alloys that we have studied. We think that the reason for the difference in behaviour between the Cr–Os and Cr–Ir systems is due to the fact that Butylenko's [18] measurements do not extend to high enough temperatures, only up to about 600 K that is not high enough to reach the true linear portion of the  $\rho$ – $T$  curve. In this regard it may be mentioned that  $\Delta T$  values obtained from measurements of Araj's *et al* [19] on pure Cr and on Cr–Os alloys up to about 1200 K, differ markedly from the results obtained by Butylenko [18]. For pure Cr Butylenko's [18] results give,  $\Delta T \approx 30$  K while they found a peak value of  $\Delta T \approx 135$  K near 0.2% Os, levelling off to a value  $\Delta T \approx 50$  K at 0.5 at.% Os. From the work of Araj's *et al* [19] we obtained, for pure Cr,  $\Delta T \approx 340$  K, and for a sample containing 0.3 at.% Os (the only sample that they studied in the range 0–0.5 at.% Os),  $\Delta T \approx 360$  K. These two values are much larger than those obtained, by Butylenko [18] and show a roughly constant  $\Delta T$  value in the range 0 to 0.3 at.% Os, in contrast with Butylenko's [18] results.

## 5. Conclusions

Electrical resistivity measurements on dilute Cr–Ir alloy single crystals show well defined magnetic anomalies at the Néel point. These anomalies become more pronounced as the Ir content is increased. A small anomaly, with hysteresis of about 20 K, is observed at the ISDW–CSDW magnetic phase transition of the Cr + 0.20 at.% Ir alloy single crystal. It is absent at the ISDW–CSDW phase transition of the Cr + 0.25 at.% Ir alloy crystal. Its absence in this latter crystal is probably due to the combined effects of sample inhomogeneities and to the finding in the present study that the parts of the Fermi surface sheets that are annihilated on the formation of the SDW state are nearly the same for ISDW and CSDW alloys. This probably also explains the absence of a resistivity anomaly in the resistivity measurements of other authors [6, 7] on Cr–Ir alloys. Analyses of the electrical resistivity data show that an extra magnetic contribution,  $\rho_m$ , to the electrical resistivity,  $\rho$ , persists in the Cr–Ir alloys up to temperatures as high as approximately  $2.5T_N$ , with a peak value at the Néel temperature,  $T_N$ . The resistivity component  $\rho_m$  is thought to originate from spin-fluctuation effects.  $\rho_m$  contributes between 20% and 25% to the total resistivity of the Cr–Ir alloys at  $T_N$ . This is about twice the contribution found previously in another dilute

Cr alloy system, namely in Cr–Ti alloys [11]. At  $T < T_N$ , the data also show a contribution from  $\rho_m$ , but the rate at which this contribution dies out on lowering  $T$  is strongly dependent on the adjustable parameter used in the analyses, pointing to inadequacies in the theoretical model.

### Acknowledgment

Financial aid from the South African Foundation for Research Development is acknowledged.

### References

- [1] Fawcett E, Alberts H L, Galkin V Yu, Noakes D R and Yakhmi J V 1994 *Rev. Mod. Phys.* **66** 25
- [2] Fawcett E 1988 *Rev. Mod. Phys.* **60** 209
- [3] Jayaraman A, Rice T M and Bucher E 1970 *J. Appl. Phys.* **41** 869
- [4] Butylenko A K and Nevdacha V V 1980 *Dokl. Akad. Nauk Ukr. SSR A* **5** 67 (in Russian)
- [5] Smit P and Alberts H L 1993 *J. Phys.: Condens. Matter* **5** 6433
- [6] de Young T F, Arajs S and Anderson E E 1971 *AIP Conf. Proc.* **5** 517
- [7] Yakhmi J V, Gopalakrishnan I K and Iyer R M 1983 *J. Less-Common Met.* **91** 327
- [8] Arajs S, Reeves N L and Anderson E E 1971 *J. Appl. Phys.* **42** 1691
- [9] Yakhmi J V, Gopalakrishnan I K and Iyer R M 1987 *J. Appl. Phys.* **61** 3994
- [10] McWhan D B and Rice T M 1967 *Phys. Rev. Lett.* **19** 846
- [11] Chiu C H, Jericho M H and March R H 1971 *Can. J. Phys.* **49** 3010
- [12] Anderson R A, Alberts H L and Smit P 1993 *J. Phys.: Condens. Matter* **5** 1733
- [13] Nye J F 1957 *Physical Properties of Crystals* (Oxford: Clarendon) pp 4, 22
- [14] Boshoff A H, Alberts H L, du Plessis P de V and Venter A M 1993 *J. Phys.: Condens. Matter* **5** 5353
- [15] Mühlischlegel B 1959 *Z. Phys.* **155** 313
- [16] Mott N F and Jones H 1958 *The Theory of the Properties of Metals and Alloys* (New York: Dover) p 274
- [17] Alberts H L 1990 *J. Phys.: Condens. Matter* **2** 9707; 1996 private communication
- [18] Butylenko A K 1985 *Sov. Phys.–Tech. Phys.* **30** 942
- [19] Arajs S, de Young T F and Anderson E E 1970 *J. Appl. Phys.* **41** 1426